Photoluminescence of TiO2: Effect of UV Light and Adsorbed Molecules on Surface Band Structure

ARTICLE *in* JOURNAL OF THE AMERICAN CHEMICAL SOCIETY · NOVEMBER 2011

Impact Factor: 12.11 · DOI: 10.1021/ja2072737 · Source: PubMed

4 AUTHORS, INCLUDING:

Ana Stevanovic
National Institute of Standards and Technology
7 PUBLICATIONS **52** CITATIONS

JACS
JOURNAL OF THE AMERICAN CHEMICAL SOCIETY
Article
pubs.acs.org/JACS

Photoluminescence of TiO_2: Effect of UV Light and Adsorbed Molecules on Surface Band Structure

Ana Stevanovic, Michael Büttner, Zhen Zhang, and John T. Yates, Jr.*

Department of Chemistry, University of Virginia, Charlottesville, Virginia 22904, United States

ABSTRACT: The photoluminescence (PL) of TiO_2 at 529.5 nm (2.34 eV) has been found to be a sensitive indicator of UV-induced band structure modification. As UV irradiation occurs, the positive surface potential changes and shifts the depth of the depletion layer. In addition, reversible band bending due to the adsorption of the electron-donor NH_3 and CO molecules has been observed in measurements combining PL with FTIR surface spectroscopy. It has been found that the O_2 molecule acts in two ways: as a reversibly adsorbed electron-acceptor molecule and as an irreversibly adsorbed molecule that heals natural oxygen vacancy defects in the near-surface region.

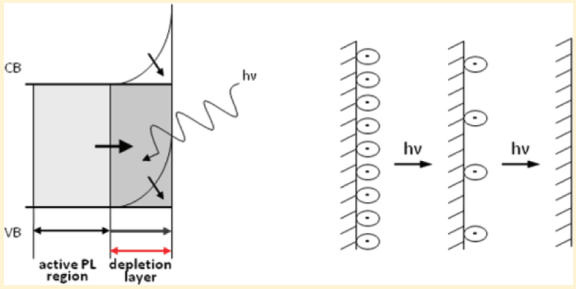

1. INTRODUCTION

Titanium dioxide is vital for solar-driven technologies such as sunlight-activated environmental remediation for photodegradation of toxic materials.[1,2] Also, photovoltaic cells based on TiO_2 are widely used.[3,4] Titanium dioxide has a band gap of 3.0−3.2 eV that permits activation by the UV component of sunlight. An electron/hole (e^-/h^+) pair is produced. The hot electron quickly relaxes to the bottom of the conduction band, where its mobility can carry it to a defect site or elsewhere. The presence of defects or impurities perturbs the local band structure of TiO_2 and breaks the periodicity of the lattice. Defects generate a local charge anomaly and thus act as traps of photogenerated electrons and holes.[5] At low temperatures, as employed in this work, the interactions between photoexcited charge carriers and lattice phonons are significantly reduced, and as a result, charge carriers become trapped at defect sites, where they recombine and emit photoluminescence (PL) or heat.[6−8] The energy of the emitted photon depends on the band structure and defect-site energies in the material.

Ellis and co-workers[9,10] first suggested that the variation in PL intensity by the adsorption of charge-donating molecules on an n-type semiconductor could alter the surface band structure of the semiconductor by reducing the depletion width as donor molecules are adsorbed. This concept builds on earlier investigations,[11] where the effects of band bending in changing the depth of the depletion layer in semiconductors were observed to affect the PL intensity, since the depletion layer is a dead layer for e^-/h^+ pair recombination processes leading to PL. The idea that donor or acceptor molecules could influence PL in TiO_2 as a result of changes in the thickness of the dead layer due to band bending was developed by Anpo and co-workers.[12,13] In addition, Solomon et al.[14] and Dunstan[15] suggested that UV irradiation alters the band bending in amorphous silicon, flattening the band through recombination of photoexcited electrons and naturally present positive charge at or near the surface. In contrast to recombination in the bulk, work by McHale and co-workers[16] identified a PL band at ∼530 nm in TiO_2, in agreement with our measurements, and they ascribed this PL emission to recombination of a mobile electron with a trapped hole on the TiO_2 surface, where the TiO_2 is in contact with solvents.

This paper considers the effect of UV light on the surface band structure of TiO_2 particles in high vacuum or following controlled gas adsorption. We have found that the PL effect is enhanced by exposure to UV light, which ultimately converts n-type TiO_2 to a flat-band condition as a result of changes in the surface photovoltage. In addition, the PL intensity can be modified by adsorbates that exchange charge with TiO_2, producing a change in the surface band-bending structure. We have also found that O_2 adsorption irreversibly reduces the concentration of natural defects in the surface region of TiO_2 particles, reducing the PL intensity. It is likely that these defects are oxygen vacancies or Ti^{3+} sites at very low concentration.

2. EXPERIMENTAL SECTION

The experiments reported here involved the use of a special spectroscopic cell in which both PL and transmission FTIR spectroscopy could be applied to a powdered TiO_2 sample (Figure 1A). The high-vacuum cell, which was connected to a small portable high-vacuum pumping system on wheels, could be moved between a purged IR spectrometer (PerkinElmer Spectrum 100) and a nearby PL spectrometer (PerkinElmer LS-55) and accurately repositioned in each spectrometer. The stainless steel IR/PL vacuum cell contained two CaF_2 windows of 23 and 48 mm diameter that were used for IR and PL measurements, respectively. The powdered TiO_2 sample was pressed at 6000 psi as a 7 mm diameter disk of thickness 0.0076 cm into a tungsten grid containing 0.22 mm × 0.22 mm square

Received: August 5, 2011
Published: November 21, 2011

   dx.doi.org/10.1021/ja2072737 | J. Am. Chem.Soc. 2012, 134, 324−332

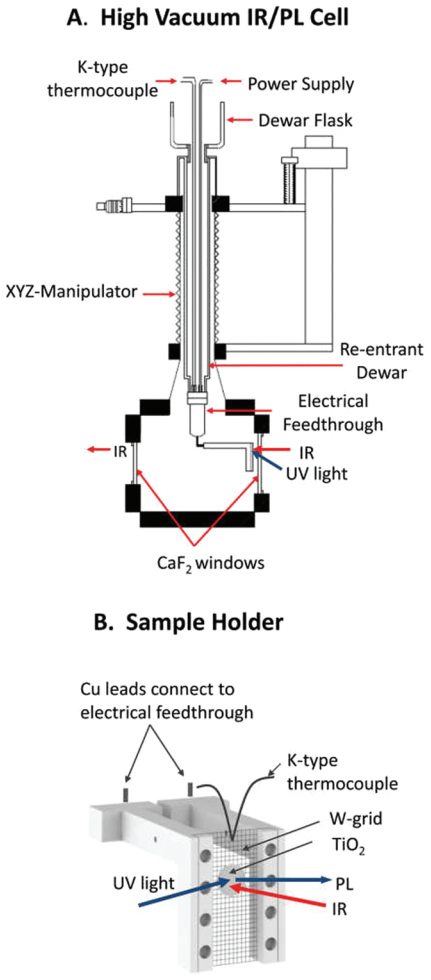

Figure 1. (A) Stainless steel IR/PL high-vacuum cell for the PL and FTIR measurements. (B) Sample holder (OFHC Cu) with clamped tungsten grid and pressed-powder TiO_2 disk.

grid openings, as shown in Figure 1B. The optical transparency of the empty grid was ~70%. The grid assembly was stretched between two oxygen-free high-conductivity (OFHC) Cu clamps that were attached to a reentrant liquid N_2 Dewar at the end of an electrical feedthrough, as shown in Figure 1B. Temperature was measured with a type-K thermocouple welded to the top center of the grid, and the grid could be programmed upward and downward in temperature using a PID controller (Eurotherm 2404).[17] The temperature range was 87−1000 K (±1 K accuracy), and the closely spaced grid wires in the powdered sample allowed uniform temperatures to be achieved across the sample.[18] The cell was pumped with a Leybold 150 turbopump and could achieve a limiting pressure of 6×10^{-9} Torr after a mild bakeout. Pressure was measured with a cold-cathode ionization gauge or a quadrupole mass spectrometer (SRS model RGA 200).

FTIR transmission measurements were carried out in the range 4000−1000 cm^{-1} using 128 scans at 2 cm^{-1} resolution. The spectrometer employed a mercury cadmium telluride (MCT) detector at 77 K. FTIR measurements through the sample were made in ratio mode by comparison to measurements made through the empty grid.

PL measurements were made using a pulsed Xe source operating at 60 Hz with a pulse width of <10 μs. During measurements, continuous exposure to the pulsed incident radiation took place unless a shutter was used to block the radiation. The measured power at the sample[19] averaged over time was 9.1×10^{-5} J s^{-1} cm^{-2} (1.5×10^{14} photons cm^{-2} s^{-1}) at the incident wavelength of 320 ± 10 nm (3.88 eV), which was selected using a grating and a band-pass filter on the source side. The UV radiation was directed across the center of the sample in a rectangular region 2 mm in width (0.14 cm^2). The spectra were obtained using 15 nm slits on the source and the detector side and a scan speed of 500 nm min^{-1}. The instrument ratioed the PL signal to the pulsed source signal. The PL signal was detected by an R928 photomultiplier tube covering the 200−900 nm range. The PL signals were measured 15° off the specular direction to minimize reflection of the source light from the sample surface and CaF_2 window. A cutoff filter at 390 nm was used on the detector side to minimize further the influence of reflected source light. Single-scan PL measurements were made using 67 s exposures to the Xe source and involved a total exposure to 9.8×10^{15} photons cm^{-2}. Experiments showed that a 67 s single scan measurement of the PL only slightly modified the TiO_2 sample, as judged by the constancy of the PL signal. However, continuous irradiation using 320 nm light produced a continuous increase in PL intensity. The PL peak shape was invariant during the experiments shown here. Small changes in the sample position in the PL spectrometer caused some variation in the PL intensity.

TiO_2 powder [Evonic Industries (formerly Degussa) P-25 material] was used in all of this work. The powdered TiO_2 was ~75% anatase and ~25% rutile with average particle sizes of ~30 and ~80 nm, respectively.[20−23] The P-25 TiO_2 had a N_2 Brunauer−Emmett−Teller (BET) surface area of 49 m^2 g^{-1}.[23] The mass of the sample was 6.3×10^{-3} g. Thus, in the 1 cm^2 geometrical area exposed to UV, ~4×10^{18} surface sites within the depth (0.0076 cm) of the sample were exposed to gas during adsorption. Since UV irradiation at 320 nm has an absorption depth of 12−25 nm in bulk rutile[24−28] and ~17 nm in anatase,[26] ~2×10^{15} surface sites cm^{-2} in the nominal penetration depth were involved in adsorption within the depth of PL emission. Thus, within the approximations used here, ~0.1 photon (surface TiO_2 site)$^{-1}$ s^{-1} was incident during the PL measurements.

For cleaning, the TiO_2 was heated in vacuum to 700 K, and 0.12 Torr O_2 was introduced for 30 min for removal of surface impurities and partial oxidization of the sample. The sample was then evacuated for 30 min at 700 K. Research-grade O_2 (99.99%), NH_3 (99.99%), and CO (99.99%) were used for adsorption in the experiments presented here.

3. EXPERIMENTAL RESULTS

A. IR Spectrum of TiO_2. Figure 2 shows the IR spectrum of the as-received TiO_2 material and the material after O_2 and vacuum treatment for 1 h at 700 K and cooling to 87 K in vacuum. Both spectra were acquired at 87 K. Originally, the TiO_2 powder (as-received) contained adsorbed isolated Ti−OH groups on the surface. The O−H stretching modes showed several different sharp absorption bands in the range 3750−3400 cm^{-1} which indicate the presence of different types of isolated Ti−OH groups on the surface.[29,30] Hydrogen bonding between OH groups at high surface coverages produces a broad low-frequency band that was not observed here. In addition, saturated hydrocarbons were present on the surface, as indicated by C−H stretching modes at 2956, 2925, and 2854 cm^{-1}. After the cleaning procedure in O_2, the TiO_2 surface

dx.doi.org/10.1021/ja2072737 | J. Am. Chem.Soc. 2012, 134, 324−332

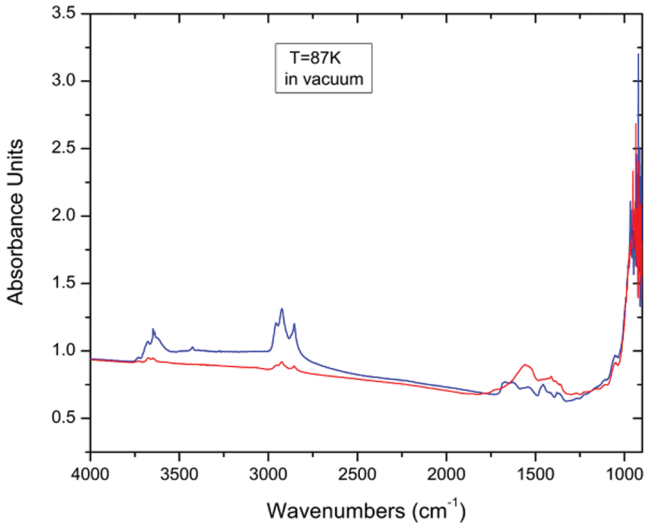

Figure 2. IR spectra of "as received" (blue) and clean (red) TiO_2 powder at 87 K in vacuum. The clean surface was obtained by treating the sample at 700 K in an oxygen atmosphere. The IR spectrum remained invariant over the experiments reported here.

contained a very small fraction of Ti−OH- and C−H-bearing species, as estimated by the low absorbances in Figure 2. Adsorbed carbonate (CO_3^{2-}) on the surface, yielding modes in the 1300−1800 cm^{-1} region, originated from CO_2 adsorption on the TiO_2 surface. The IR spectrum of the prepared sample remained unchanged throughout the experiments shown here.

B. PL Development during UV Irradiation. Figure 3A shows the PL development during continuous UV irradiation in vacuum at 87 K. The sample was irradiated at λ = 320 nm (3.88 eV). The PL intensity maximum occurred at λ = 529.5 nm (2.34 eV) and increased as UV radiation was continuously absorbed. Two spurious peaks were observed at 390 and 780 nm, respectively. The peak at λ = 390 nm is due to a small amount of reflected source radiation, and its intensity remained constant during irradiation as the PL developed. The peak at 780 nm is a second-order feature of the 390 nm reflected light and also remained constant during irradiation. It was also weakly seen in the reference spectrum measured for the clean grid support (blue line). Figure 3B shows a plot of the increasing PL peak maximum intensity from the data in Figure 3A as a function of UV irradiation time. After the sample was irradiated for ∼160 min, the UV light was blocked for ∼60 min, and then the sample was irradiated again for ∼90 min. The PL peak intensity produced by UV irradiation remained essentially unchanged [region (b) in Figure 3B] when the TiO_2 was stored for ∼60 min in the dark in vacuum. Storage of charge on irradiated TiO_2 surfaces has been observed previously.[31,32] Under the vacuum conditions employed here, any trace of adsorbed background gas not measured by IR spectroscopy did not change the PL efficiency. The enhancement of PL continued when the sample was irradiated again in vacuum after storage in the dark at 87 K, as shown beyond 220 min in region (c) in Figure 3B. This experiment shows that the increasing PL intensity produced by UV irradiation corresponds to the production of a stable surface condition at 87 K in vacuum. In addition, the absorption spectrum of TiO_2 (not shown) indicated no evidence for an absorption band in the frequency range of the PL emission.

C. PL Enhancement. Figure 4A indicates the change in PL intensity during UV irradiation at different photon fluxes. Three otherwise identical experiments were performed with 100, 70, and 40% of the full photon flux, using neutral density grids to reduce the incident photon intensity. The TiO_2 powder was irradiated for ∼216 min in vacuum at 87 K. In all three experiments, the PL intensity increased with time and approached a saturation level. Two important observations may be made: (1) the increase in PL intensity is a result of exposure of the material to incident UV light (process k_1), and (2) a saturation condition is achieved after long irradiation. In addition, Figure 4A shows that when the incident UV photon flux was reduced, the PL generation rate decreased, achieving the saturation point more slowly.

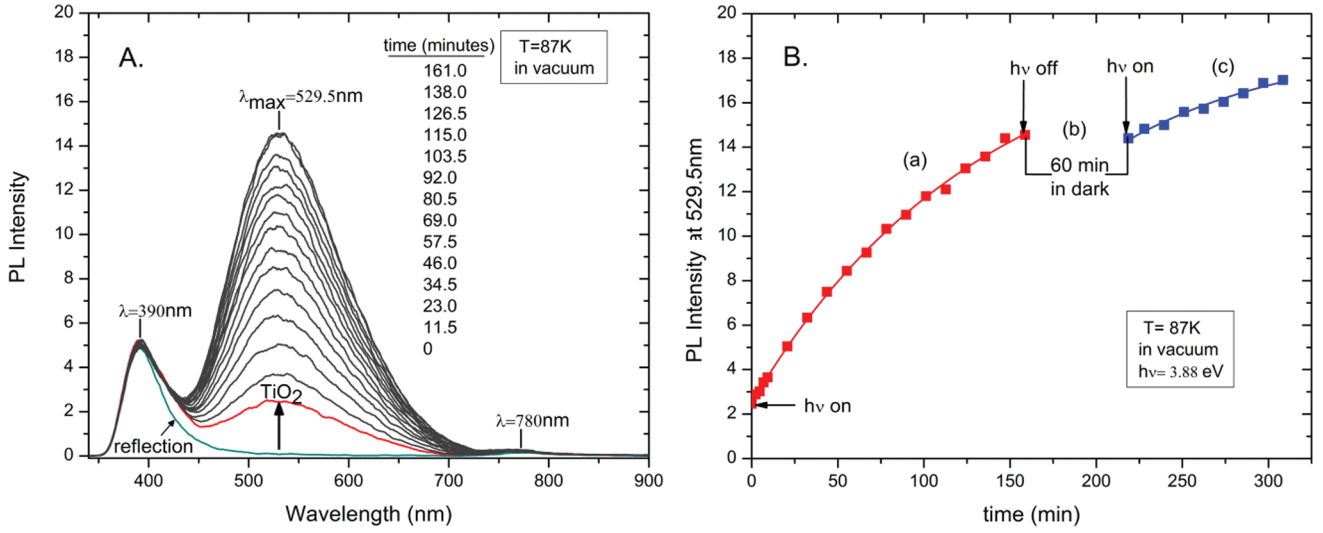

Figure 3. (A) PL development for TiO_2 during irradiation in vacuum. The reference spectrum, obtained using a clean W grid at the sample position, is shown by the blue line. (B) Increase in PL intensity of TiO_2 as a function of UV exposure at 87 K in vacuum: (a) The sample was irradiated at λ = 3.88 eV for 160 min (red curve). The PL intensity increased with irradiation time as the number of photon-accessible defects increased. (b) The sample was stored in the dark in vacuum for 60 min. (c) The sample was irradiated again at λ = 3.88 eV for 90 min (blue curve). The PL remained constant when the UV light was off (∼60 min) and continued to increase when the UV light was on.

dx.doi.org/10.1021/ja2072737 | J. Am. Chem.Soc. 2012, 134, 324−332

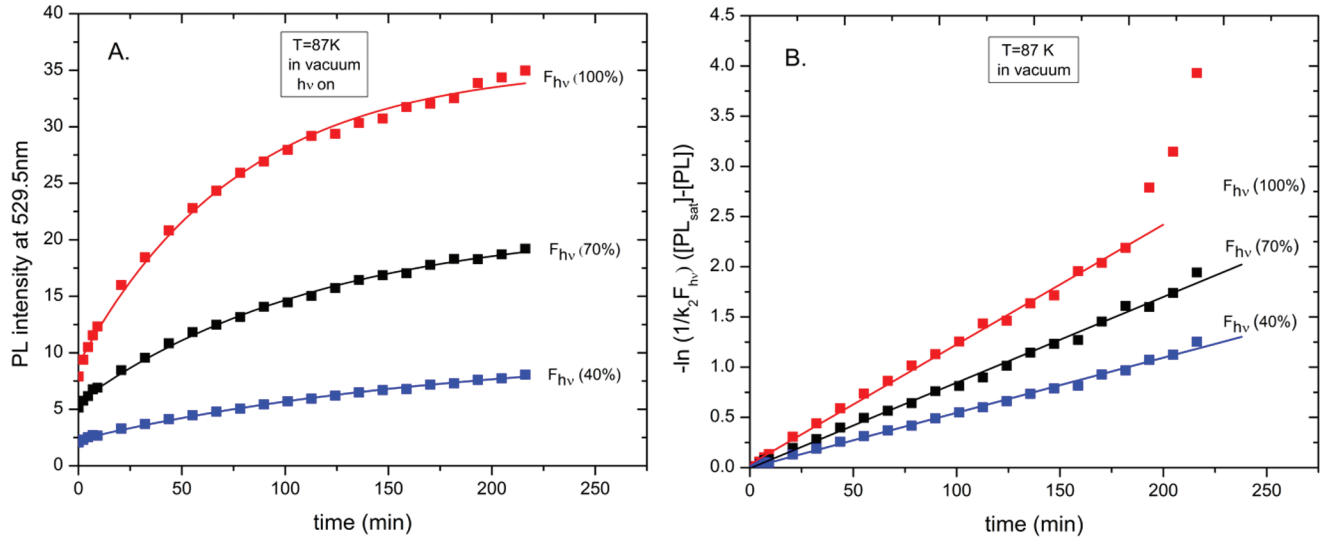

Figure 4. (A) PL intensity of TiO_2 as a function of time at different photon fluxes ($F_{h\nu}$): 100% (red), 70% (black), and 40% (blue). The rate of production of photon-accessible defects decreases as the light intensity decreases. (B) Functional fits of the PL intensity development during irradiation at different $F_{h\nu}$: 100% (red), 70% (black), 40% (blue). Solid squares represent experimental data. All data sets were fit using eqs 3 and 5, and the fits are shown as solid lines.

Charging the surface by exposure to UV photons alters the surface potential (photovoltage) and the degree of band bending and hence produces changes in the depth of the depletion region. Accumulation of positive charge on an n-type semiconductor surface (decrease in work function) decreases upward band bending, leading to a flat-band structure and resulting in the saturation of the PL intensity as the length of the depletion region decreases to zero.

On the basis of these observations, the effect can be described by a model wherein 1 cm^2 of surface area is considered. UV irradiation induces a reduction in surface charge that enhances the PL as a result of the reduction in upward band bending in the n-type semiconductor; the PL intensity is proportional to the active defect concentration [D] (cm^{-3}) averaged over the entire depth of light penetration in an individual TiO_2 particle. A natural saturation is achieved at long UV exposure times, when the band bending is reduced to zero. Therefore, the change in the photon-accessible defect concentration during UV exposure can be described by the following equation:

$$\frac{d[D]}{dt} = k_1 F_{h\nu}([D]_{sat} - [D]) \quad (1)$$

where [D] is the PL-active defect concentration, expressed as the average concentration of the photon-accessible defects over the active PL region and the dead region considered together; k_1 is the rate constant for photon-accessible defect production; $F_{h\nu}$ is the photon flux at 3.88 eV; and $[D]_{sat}$ is the upper limit of photon-accessible defect concentration available for PL. At any time, the quantity ($[D]_{sat} - [D]$) is equal to the photon-accessible defect concentration, which may be developed by irradiation until saturation.

For the PL rate, we may write

$$[PL] = k_2 F_{h\nu}[D] \quad (2)$$

where k_2 is proportionality constant for PL and [PL] denotes the intensity of the 2.34 eV PL.

From eqs 1 and 2, the PL intensity development during UV irradiation can be obtained:

$$[PL] = k_2 F_{h\nu}[D]_{sat} - k_2 F_{h\nu} e^{-k_1 F_{h\nu} t} \quad (3)$$

which rearranges to

$$\ln\left([D]_{sat} - \frac{1}{k_2 F_{h\nu}}[PL]\right) = -k_1 F_{h\nu} t \quad (4)$$

Since

$$[D]_{sat} = \frac{[PL]_{sat}}{k_2 F_{h\nu}}$$

we obtain

$$\ln\left[\frac{1}{k_2 F_{h\nu}}([PL]_{sat} - [PL])\right] = -k_1 F_{h\nu} t \quad (5)$$

Equation 5 accurately fits the experimental data in Figure 4, including the scaling with $F_{h\nu}$, as shown by the line fits to the points in Figure 4A,B. Figure 4B shows the dependence of the PL intensity on the photon flux as the logarithmic function derived in eq 5. The slopes of the curves are directly proportional to $F_{h\nu}$ of the incident light. The deviation of a few points on the upper plot from the linear dependence at $F_{h\nu}$ = 100% is probably due to some small experimental error.

D. Annealing Effect. Figure 5 shows that the PL intensity decreased as the annealing temperature (T_a) was increased in vacuum following near saturation of the photon-available defect concentration by UV irradiation. After each annealing process, the PL increased again with increasing exposure to UV radiation. The sample was annealed from 87 K to T_a and then cooled back down to 87 K. All of the PL measurements were performed at 87 K. This observation is consistent with an irreversible thermal effect that removes the flat-band condition previously established by irradiation. We have no explanation for this effect at present.

E. Effect of NH_3 Adsorption. Following the photoproduction of a near-saturated level of photon-accessible defects able to cause e^-/h^+ recombination (flat-band condition), donor NH_3 molecules were adsorbed on the

dx.doi.org/10.1021/ja2072737 | J. Am. Chem.Soc. 2012, 134, 324–332

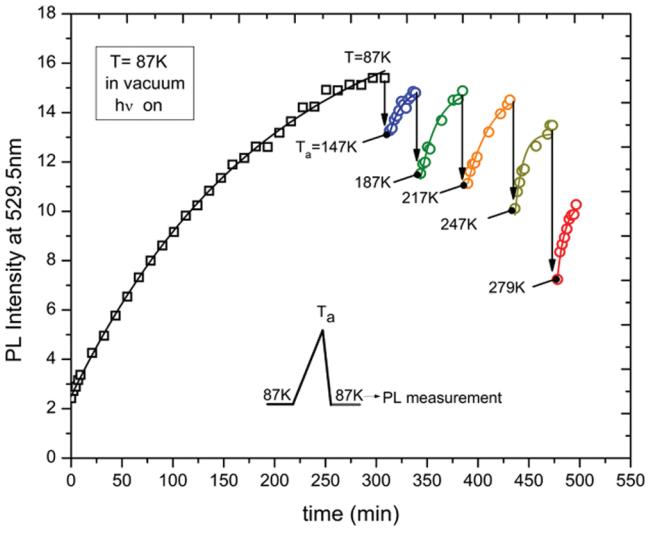

Figure 5. PL intensity decrease with increasing annealing temperature in vacuum. The sample was annealed from 87 K to T_a and then cooled back down to 87 K. All of the PL measurements were performed at 87 K. After annealing in vacuum, continuous irradiation causes PL enhancement.

TiO_2 at 200 K. As shown in Figure 6, the first dose of NH_3 decreased the PL intensity immediately, and subsequent NH_3

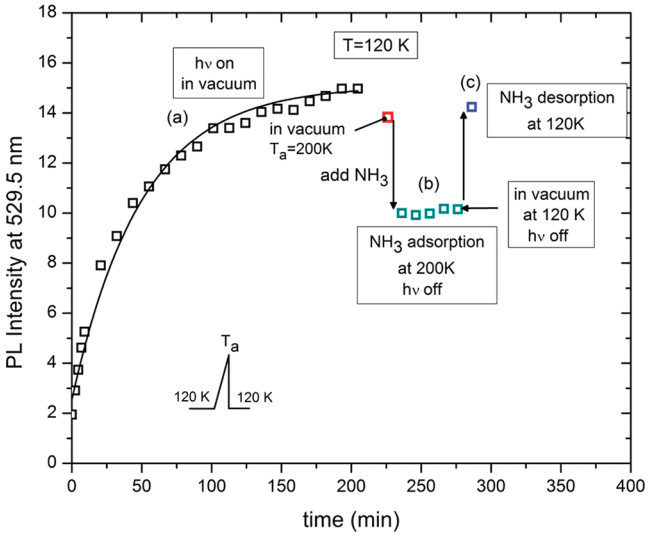

Figure 6. Effect of NH_3 adsorption and desorption on the PL intensity following production of positive surface charge by irradiation. Adsorption (200 K) and desorption (120 K) occurs rapidly in the near-surface region of the powdered layer upon excitation by UV irradiation.

doses had no additional effect [region (b)]. Upon evacuation at 120 K, the PL intensity immediately returned to near its initial value [region (c)]. This is evidence that the reversible adsorption/desorption of NH_3 on the outer TiO_2 surface regions is being probed by PL. The adsorption of NH_3 was observed by IR spectroscopy for the exposures used here at 200 K (data not shown). All of the PL measurements following NH_3 adsorption at 200 K (Figure 6) were made after adsorption at 200 K and then cooling to 120 K. It may be seen that perfectly *reversible* behavior is observed as the PL responds to adsorbed NH_3. This is in accordance with the development of a surface potential moving in the negative direction for NH_3 adsorption on a flat-band condition achieved by prior irradiation. Adsorption results in downward band bending, consistent with the known behavior of NH_3 as a donor molecule.

F. Effect of CO Adsorption. As shown in Figure 7, carbon monoxide was adsorbed at 120 K on an irradiated sample

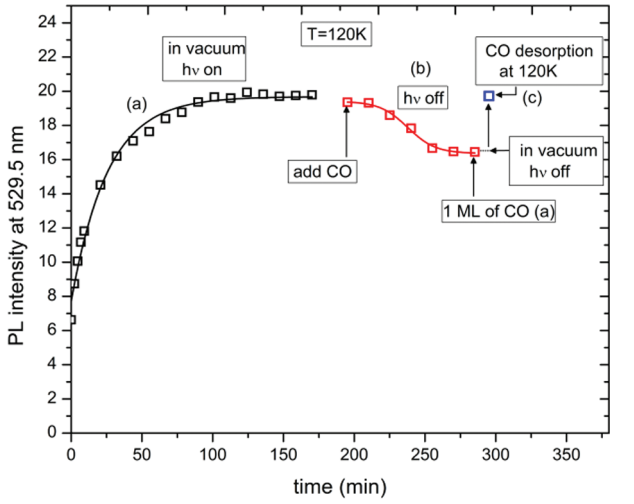

Figure 7. (a) PL evolution during continuous UV exposure in vacuum (black curve). (b) Change in PL intensity during CO adsorption until saturation coverage was attained (as judged by IR) in the dark at 120 K (red curve). (c) Reversible recovery of the PL intensity after the system was evacuated in the dark at 120 K (blue □).

showing initially a near-maximum PL intensity [region (a)]. CO adsorption was carried out in region (b). An absorption band at $\nu(CO) \approx 2180$ cm^{-1}, accompanied by a small IR feature at $\nu(CO) \approx 2165$ cm^{-1}, was observed to develop (data not shown). Since these frequencies are above the gas-phase $\nu(CO_{(g)})$ frequency of ~2143 cm^{-1}, the CO molecule behaved as a weak donor molecule. The PL intensity decreased as CO was adsorbed [region (b)]. As desorption of the CO occurred after the cell was evacuated back to high vacuum at ~120 K, the PL was restored, and its intensity returned to the value originally achieved by irradiation. These results indicate that CO also acts as a donor molecule, resulting in downward band bending from the initial flat-band condition. The PL responds *reversibly* to the adsorption/desorption of CO. This observation is consistent with the development of a surface potential moving in the negative direction upon CO adsorption.

G. Effect of O_2. Figure 8 shows the change in PL intensity during UV irradiation in the presence of O_2(g). It shows a suppression of the PL enhancement rate with increasing O_2 pressure at 120 K for continuous exposure to UV light. In other words, the UV-light-induced PL intensity enhancement is inhibited by O_2 at 120 K. No change in PL intensity was observed in region (b) after the system was evacuated back to high vacuum and stored in the dark for ~15 min, implying that the surface condition (produced by UV irradiation at low O_2 pressures at 120 K) is stable in vacuum in the dark. This is in agreement with a similar observation at 87 K, as shown in region (b) in Figure 3B. In addition, when the sample was continuously UV-irradiated again in vacuum, the PL intensity increased as a result of the continued formation of a negative

dx.doi.org/10.1021/ja2072737 | J. Am. Chem.Soc. 2012, 134, 324–332

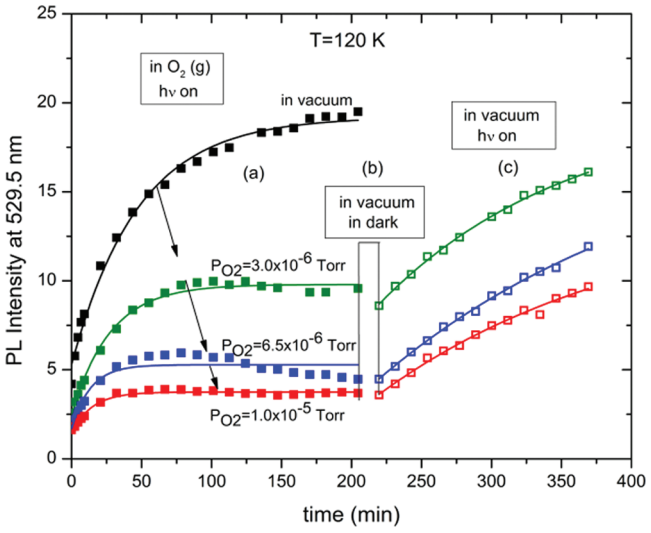

Figure 8. PL intensity development during irradiation when low pressures of O_2(g) are present. (a) PL development in vacuum (black) and in O_2 atmosphere (green, 3.0×10^{-6} Torr; blue, 6.5×10^{-6} Torr; red, 1.0×10^{-5} Torr). (b) No change in PL intensity occurred in the dark in vacuum for 15 min. (c) The PL intensity increased again in vacuum upon exposure to UV irradiation.

surface potential by UV irradiation in the absence of O_2 [Figure 8, region (c)].

Region (b) in Figure 9A shows the change in PL intensity caused by O_2 adsorption in the dark at 120 K after the maximum PL intensity was first achieved by irradiation. The PL intensity smoothly decreased [inset (e)] after the introduction of increasing O_2 pressures (P_{O_2}). The initial and final O_2 pressures were 1.5×10^{-2} and 3 Torr, respectively. The UV light was blocked between O_2 doses in region (b). These results indicate that the PL intensity at 120 K is extremely sensitive to the presence of O_2 molecules, which cause a decrease in PL. This effect is related to the production of weakly adsorbed O_2 in equilibrium with gas-phase O_2,[33] which is a precursor to the chemisorption of O_2. The PL intensity decreased quickly when the TiO_2 was exposed to small pressures of O_2 (1.5×10^{-2} to 4.0×10^{-1} Torr) and reached a minimum at ~3 Torr at 120 K. After O_2(g) was pumped away [region (c)], the PL intensity rose immediately as weakly bound O_2 desorbed. Following the abrupt O_2 desorption in region (c), the PL showed the previously observed effect (an increase in PL intensity) as the sample was further irradiated with UV light in vacuum. Region (a) in Figure 9B shows the change in PL intensity achieved by UV exposure in vacuum. Region (b) shows the PL behavior after O_2 adsorption at 113 K in the dark. After each O_2 dose (0.1, 0.5, 5.0, and 9 Torr), the PL was recorded as a function of time. The UV light was always kept on between the measurements, in contrast to the experiments shown in Figure 9A. The PL intensity decreased dramatically when the first O_2 dose (0.1 Torr) was in contact with the surface. The PL intensity remained almost unchanged in the presence of O_2 at various high values of P_{O_2} during UV irradiation. This shows that at sufficiently high P_{O_2}, UV irradiation cannot cause enhancement of the PL. The small decrease in PL intensity for increasing P_{O_2} is probably due to the slight TiO_2 sample warming as higher O_2(g) pressures were used, caused by heat transfer to the sample from the cell walls at 300 K.

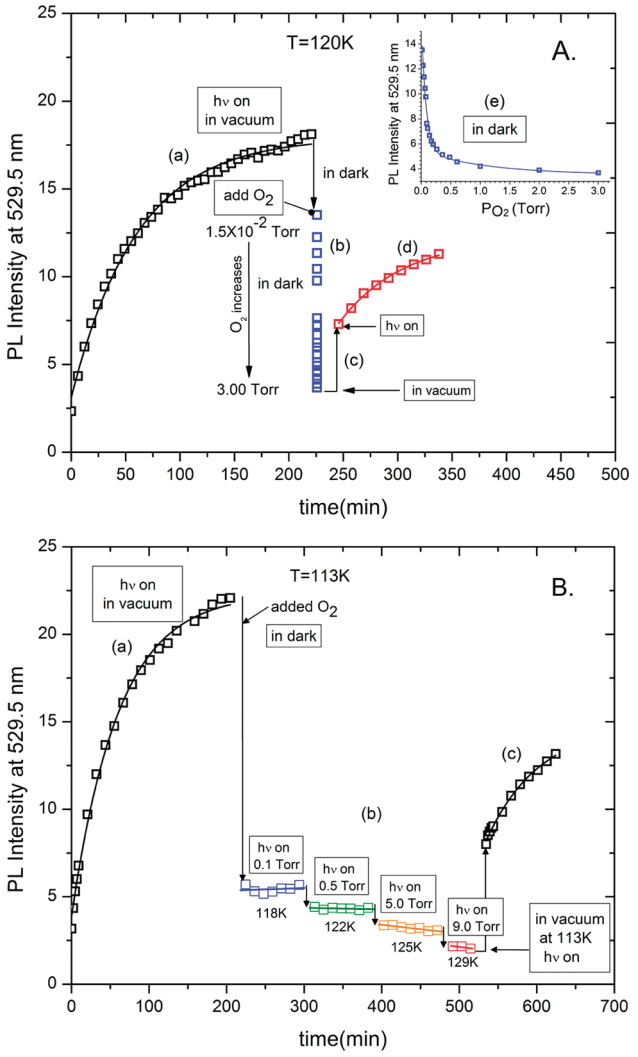

Figure 9. (A) (a) PL development in vacuum during continuous radiation (black □). (b) PL intensity after the introduction of different amounts of O_2 in the dark (blue □), plotted at the same time. The inset (e) depicts the PL intensity decrease in the dark as a function of P_{O_2}. (c) Increase in PL intensity due to O_2 desorption upon evacuation of O_2 in the dark. (d) Increase in PL with continuous irradiation in vacuum (red □). (B) (a) PL development during exposure to UV irradiation at 113 K in vacuum (black □). (b) Different partial pressures of O_2 were introduced (blue, 0.1 Torr; green, 0.5 Torr; orange, 5.0 Torr; red, 9.0 Torr). After each oxygen dose, the PL was recorded at the shown P_{O_2} as a function of time. Continuous UV irradiation occurred between the measurements. (c) PL increase upon evacuation due to O_2 desorption and during continuous irradiation in vacuum (black □).

Comparing these results with those obtained in the adsorption of NH_3 and CO, one can see that while O_2 behaves as an acceptor molecule as expected, causing the PL to decrease, as it bends the flattened surface band upward, *it does not behave completely reversibly* as do NH_3 and CO. The same oxygen behavior was observed by Anpo et al.[34] in ZnO powder. It is likely that O_2 also irreversibly heals TiO_2 defect sites (oxygen vacancies or Ti^{3+} interstitials) that are naturally present in the sample. The healing of these defects causes a reduction in the PL intensity because of the linear dependence of PL on the defect concentration.

dx.doi.org/10.1021/ja2072737 | J. Am. Chem.Soc. 2012, 134, 324–332

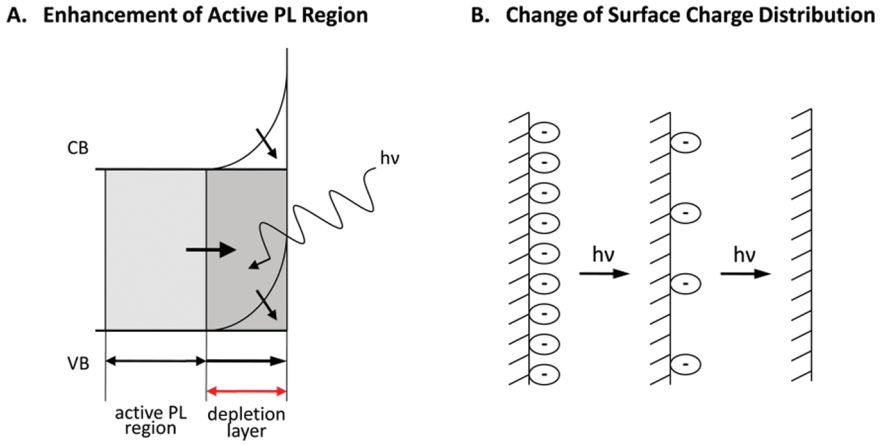

Figure 10. Schematic illustration of the effect of UV irradiation on n-type TiO_2. The flattening of the band is associated with a reduction of surface negative charge during irradiation. The process culminates when a flat-band condition is achieved.

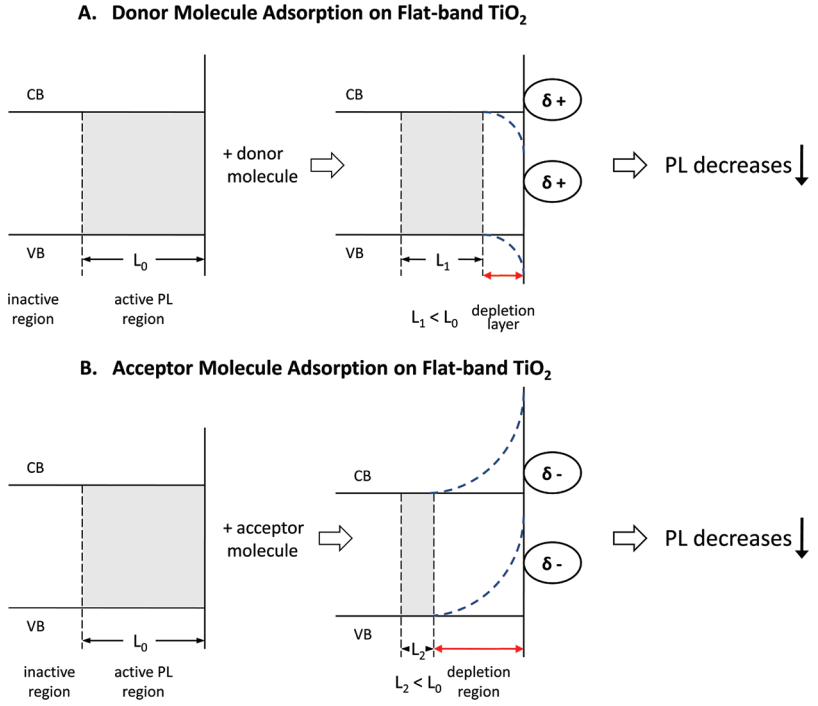

Figure 11. Schematic effect of donor and acceptor molecules on the thickness of the active PL region. (A) TiO_2 with the flat-band condition achieved by maximum UV exposure in vacuum. The active PL region length is L_0. Upon adsorption of an electron-donor molecule, the length of active PL region decreases to L_1, where $L_1 < L_0$, resulting in a decrease in PL intensity. (B) After adsorption of an electron-acceptor molecule, the length of the active PL region narrows to L_2 ($L_2 < L_0$), leading to a decrease in PL intensity.

4. DISCUSSION

A. Surface Potential Changes during UV Irradiation of TiO_2. The fundamental premise of this work is that the enhancement of PL during exposure of TiO_2 to a flux of UV radiation (3.88 eV) produces a change in the concentration [D] of photon-accessible defects, which then serve to mediate e^-/h^+ pair recombination to produce PL, as originally suggested by Solomon[14] and Dunstan.[15] A model involving band bending due to surface photovoltage changes provides a conceptual framework, where the length of the depletion layer in the region of the bent band profile changes as UV irradiation occurs, causing the number of photon-available defect sites for recombination in the flat-band region to vary. Changes due to the surface photovoltage effect cause changes in the concentration of photon-accessible defect sites, [D], expressed as an average over the depth of the surface of individual TiO_2 particles that is penetrated by UV radiation. PL can only occur deeper in the semiconductor beneath the dead-layer depletion region, since carriers are swept away from each other in the depletion region. The depth of penetration of UV irradiation with photon energy above the band-gap energy has been reported to be in the range 12−25 nm for bulk TiO_2,[24−28] and the number of defect sites within the flat-band region in the 12−25 nm photon penetration depth therefore governs the PL intensity. To provide qualitative support for the band-bending model in the nanosized particles, we used the approach outlined in ref 35 to estimate that the depth of the depletion layer in the powdered TiO_2 is ~6 nm. The estimated thickness of the depletion layer is an order of magnitude smaller than the average size of the TiO_2 particles used in this work (30−80

dx.doi.org/10.1021/ja2072737 | J. Am. Chem.Soc. 2012, 134, 324−332

nm), implying the validity of the band-bending model for our TiO_2 nanoparticles.

The generation of new photoactive sites by UV irradiation may be envisioned as in Figure 10. As photons enter the n-type TiO_2 sample, the average concentration of photoactive sites increases as the surface photovoltage decreases, and the active PL region expands toward the surface as the upward-bent band flattens (Figure 10A).

The rate of generation of photon-accessible defect sites, $d[D]/dt$, decreases as the active PL region expands, as shown by eq 1, until the rate reaches zero as $[D]_{sat}$ is achieved. As shown in Figure 10B, the normal positive surface potential of n-type TiO_2 decreases as the degree of upward band bending diminishes during irradiation.

B. Effect of Donor or Acceptor Molecule Adsorption. As shown in Figure 11, when the flat-band condition (achieved by long UV irradiation in vacuum) is modified by adsorption of either donor or acceptor molecules, the depletion region is expanded, and the number of photon-accessible defects able to facilitate e^-/h^+ recombination decreases as the surface band is bent upward or downward. The reversible response of the PL intensity caused by NH_3 and CO donor adsorbate surface modifiers is consistent with this picture of surface potential changes.

C. Irreversible Effect of Oxygen. The irreversible effect of O_2 adsorption on TiO_2 is likely superimposed on a reversible effect due to the acceptor nature of the adsorbed O_2 molecule. It is well-known that TiO_2 surfaces prepared as in this work are oxygen-deficient and therefore are n-type and possess oxygen vacancies, as observed by scanning tunneling microscopy (STM),[36] by electron spin resonance spectroscopy,[37] and theoretically.[38] Treatment with O_2, even under the mild conditions of this experiment, can alter the natural oxygen vacancy concentration at the surface and possibly in the near-surface region. Thus, on TiO_2(110), oxygen vacancy sites are observed by STM to be present at the 8% monolayer surface coverage. These surface vacancies are known to adsorb O_2 molecules[39] and serve as dissociation sites for the production of O atoms, which heal the vacancy sites as well as attaching to Ti_{5c} sites nearby.[40−43]Thus, the irreversible adsorption of O_2 and its dissociation on natural defects present in TiO_2 should be expected to result in an irreversible decrease in PL due to defect healing, as observed.

D. Possible Oxygen Vacancy Formation by UV Irradiation. STM has been used to study the possible formation of surface defects on TiO_2 (110) by UV irradiation.[44] In the photon energy range 1.6−5.6 eV, no production of defects was found for intense UV irradiation. An upper limit of the damage cross section for surface defect formation [$Q = 10^{-23.5\pm0.2}$ cm^2 photon^{-1}] was measured. At the low UV fluxes ($F_{h\nu}$) used here in the PL measurements, the measured upper limit of the TiO_2 damage cross section, Q, suggests that the maximum number of defects produced in 200 min of continuous irradiation should be less than $\sim 5 \times 10^{-6}$ times the number of available TiO_2 units in a 12−25 nm depth of UV penetration. This suggests that permanent UV-induced defect production is not involved in the PL effects reported here. Instead, the effect of band bending due to increasing surface photovoltage in governing the depth of the active PL region determines the intensity of the PL observed in these experiments.

5. SUMMARY

It has been found that alteration of the surface potential of TiO_2 by UV light or adsorbed electron-acceptor/donor molecules results in a change in the depth of the active PL region and in the intensity of the observed PL as a result of the band-bending effect. The results presented here show the following:

1. UV light induces a negative surface potential that diminishes upward band bending in n-type TiO_2 and causes the PL-active region to expand toward the surface, providing an additional number of photon-accessible defects for e^-/h^+ recombination. The increase in photon-accessible defects due to the increase in the flat-band active region results in an increase in the PL intensity. It is likely that the maximum PL intensity produced by UV irradiation results in the production of a flat-band condition at the surface.
2. Adsorption of NH_3 and CO (donor adsorbates) on the photoirradiated (flat-band) surface results in downward band bending and expansion of the depletion region, providing a lower concentration of photon-accessible defect recombination centers. As a result, the PL intensity decreases reversibly upon the adsorption of these molecules.
3. Adsorption of O_2 (acceptor adsorbate) on the photo-irradiated (flat-band) surface produces upward band bending, which also increases the depletion region and reduces the concentration of photon-accessible defect recombination centers. Thus, the PL intensity decreases reversibly upon the adsorption of O_2.
4. The PL intensity responds reversibly to NH_3 and CO adsorption/desorption. On the other hand, the PL intensity does not respond completely reversibly to O_2 desorption. This is due to the fact that in addition to being a reversibly adsorbed electron-acceptor molecule, O_2 also dissociates, causing the healing of defect sites that are naturally present in the sample.
5. The ability of PL to measure the rate of the e^-/h^+ recombination process during UV irradiation presents an opportunity to gain a deeper understanding of the exchange of charge experienced by various surface-modifier molecules upon adsorption on TiO_2. Such knowledge could be valuable in controlling processes driven by light on TiO_2 surfaces.

AUTHOR INFORMATION

Corresponding Author
johnt@virginia.edu

ACKNOWLEDGMENTS

We acknowledge with thanks the full support of this work by the Army Research Office under Grant 55748CH.

REFERENCES

(1) Thompson, T. L.; Yates, J. T. Jr. *Chem. Rev.* **2006**, *106*, 4428.
(2) Linsebigler, A. L.; Lu, G. Q.; Yates, J. T. *Chem. Rev.* **1995**, *95*, 735.
(3) Grätzel, M. *Nature* **2001**, *414*, 338.
(4) Hardin, B. E.; Hoke, E. T.; Armstrong, P. B.; Yum, J. H.; Comte, P.; Torres, T.; Fréchet, J. M. J.; Nazeeruddin, M. K.; Grätzel, M.; McGehee, M. D. *Nat. Photonics* **2009**, *3*, 406.
(5) Gfroerer, T. H. In *Encyclopedia of Analytical Chemistry*; Wiley: Chichester, U.K., 2000; p 9209.

(6) Amtout, A.; Leonelli, R. *Solid State Commun.* **1992**, *84*, 349.
(7) Najafov, H.; Tokita, S.; Ohshio, S.; Kato, A.; Saitoh, H. *Jpn. J. Appl. Phys., Part 1* **2005**, *44*, 245.
(8) Tang, H.; Prasad, K.; Sanjines, R.; Schmid, P. E.; Levy, F. *J. Appl. Phys.* **1994**, *75*, 2042.
(9) Meyer, G. J.; Lisensky, G. C.; Ellis, A. B. *J. Am. Chem. Soc.* **1988**, *110*, 4914.
(10) Winder, E. J.; Moore, D. E.; Neu, D. R.; Ellis, A. B.; Geisz, J. F.; Kuech, T. F. *J. Cryst. Growth* **1995**, *148*, 63.
(11) Hollingsworth, R. E.; Sites, J. R. *J. Appl. Phys.* **1982**, *53*, 5357.
(12) Anpo, M.; Tomonari, M.; Fox, M. A. *J. Phys. Chem.* **1989**, *93*, 7300.
(13) Anpo, M.; Chiba, K.; Tomonari, M.; Coluccia, S.; Che, M.; Fox, M. A. *Bull. Chem. Soc. Jpn.* **1991**, *64*, 543.
(14) Solomon, I.; Perrin, J.; Bourdon, B. *Proc. Int. Conf. Phys. Semicond., 14th* **1978**, 689.
(15) Dunstan, D. J. *J. Phys. C: Solid State Phys.* **1981**, *14*, 1363.
(16) Knorr, F. J.; Mercado, C. C.; McHale, J. L. *J. Phys. Chem. C* **2008**, *112*, 12786.
(17) Muha, R. J.; Gates, S. M.; Yates, J. T.; Basu, P. *Rev. Sci. Instrum.* **1985**, *56*, 613.
(18) Basu, P.; Ballinger, T. H.; Yates, J. T. *Rev. Sci. Instrum.* **1988**, *59*, 1321.
(19) We thank Dr. Y. Zong (National Institute of Standards and Technology) for assistance with measuring the photon flux of the Xe pulsed lamp using a Thorlabs energy meter (PM100D) and bolometer thermal power sensor (S302C).
(20) Jensen, H.; Joensen, K. D.; Jorgensen, J. E.; Pedersen, J. S.; Sogaard, E. G. *J. Nanopart. Res.* **2004**, *6*, 519.
(21) Li, G.; Gray, K. A. *Chem. Phys.* **2007**, *339*, 173.
(22) Martra, G. *Appl. Catal., A* **2000**, *200*, 275.
(23) Ohno, T.; Sarukawa, K.; Tokieda, K.; Matsumura, M. *J. Catal.* **2001**, *203*, 82.
(24) Ghosh, A. K.; Maruska, H. P. *J. Electrochem. Soc.* **1977**, *124*, 1516.
(25) Eagles, D. M. *J. Phys. Chem. Solids* **1964**, *25*, 1243.
(26) Mo, S. D.; Ching, W. Y. *Phys. Rev. B* **1995**, *51*, 13023.
(27) Cardona, M.; Harbeke, G. *Phys. Rev.* **1965**, *137*, A1467.
(28) Ghosh, G. *Handbook of Optical Constants of Solids*; Academic Press: San Diego, 1985.
(29) Deiana, C.; Fois, E.; Coluccia, S.; Martra, G. *J. Phys. Chem. C* **2010**, *114*, 21531.
(30) Panayotov, D. A.; Yates, J. T. Jr. *Chem. Phys. Lett.* **2005**, *410*, 11.
(31) Berger, T.; Diwald, O.; Knözinger, E.; Sterrer, M.; Yates, J. T. Jr. *Phys. Chem. Chem. Phys.* **2006**, *8*, 1822.
(32) Berger, T.; Sterrer, M.; Diwald, O.; Knözinger, E.; Panayotov, D.; Thompson, T. L.; Yates, J. T. Jr. *J. Phys. Chem. B* **2005**, *109*, 6061.
(33) Green, I. X.; Yates, J. T. Jr. *J. Phys. Chem. C* **2010**, *114*, 11924.
(34) Anpo, M.; Kubokawa, Y. *J. Phys. Chem.* **1984**, *88*, 5556.
(35) Hagfeldt, A.; Grätzel, M. *Chem. Rev.* **1995**, *95*, 49.
(36) Diebold, U.; Lehman, J.; Mahmoud, T.; Kuhn, M.; Leonardelli, G.; Hebenstreit, W.; Schmid, M.; Varga, P. *Surf. Sci.* **1998**, *411*, 137.
(37) Brandão, F. D.; Pinheiro, M. V. B.; Ribeiro, G. M.; Medeiros-Ribeiro, G.; Krambrock, K. *Phys. Rev. B* **2009**, *80*, No. 235204.
(38) Na-Phattalung, S.; Smith, M. F.; Kim, K.; Du, M.-H.; Wei, S.-H.; Zhang, S. B.; Limpijumnong, S. *Phys. Rev. B* **2006**, *73*, No. 125205.
(39) Diebold, U. *Surf. Sci. Rep.* **2003**, *48*, 53.
(40) Lira, E.; Hansen, J. O.; Huo, P.; Bechstein, R.; Galliker, P.; Laegsgaard, E.; Hammer, B.; Wendt, S.; Besenbacher, F. *Surf. Sci.* **2010**, *604*, 1945.
(41) Petrik, N. G.; Kimmel, G. A. *J. Phys. Chem. Lett.* **2010**, *1*, 1758.
(42) Scheiber, P.; Riss, A.; Schmid, M.; Varga, P.; Diebold, U. *Phys. Rev. Lett.* **2010**, *105*, No. 216101.
(43) Wang, Z. T.; Du, Y. G.; Dohnalek, Z.; Lyubinetsky, I. *J. Phys. Chem. Lett.* **2010**, *1*, 3524.
(44) Mezhenny, S.; Maksymovych, P.; Thompson, T. L.; Diwald, O.; Stahl, D.; Walck, S. D.; Yates, J. T. Jr. *Chem. Phys. Lett.* **2003**, *369*, 152.